Effect of Gln151 on L-phenylalanine feedback resistance of AroG isoform of DAHP synthase in *Escherichia coli*

Charintip Yenyuvadee, Nichaphat Kanoksinwuttipong, Kanoktip Packdibamrung[*]

Department of Biochemistry, Faculty of Science, Chulalongkorn University, Bangkok 10330 Thailand

[*]Corresponding author, e-mail: kanoktip.p@chula.ac.th

ABSTRACT: In *Escherichia coli*, 3-deoxy-D-arabino-heptulosonate-7-phosphate synthase (DAHP synthase) is the first enzyme in aromatic amino acid synthetic pathway. It consists of three isoforms, AroG, AroF and AroH, which are inhibited by L-phenylalanine, L-tyrosine and L-tryptophan, respectively. AroG, the major isoform, represents about 80% of the total DAHP synthase activity in the cells. To increase the production of L-phenylalanine in *E. coli*, it is important to reveal the inhibition mechanism of AroG and relieve the degree of inhibition. Therefore, this study aims to investigate the important amino acid residue that interacts with L-phenylalanine at the regulatory site and determine its effect on L-phenylalanine feedback inhibition. From the previously reported 3D structure of AroG co-crystallized with L-phenylalanine, Gln151 was mutated to construct L-phenylalanine feedback resistant AroG. Three mutant clones (AroG^{Q151A}, AroG^{Q151L} and AroG^{Q151N}) were prepared by using QuikChange site-directed mutagenesis. The mutated enzymes exhibited a slightly higher DAHP synthase activity than the wild type, and a decrease in percentage of inhibition by 20 mM L-phenylalanine from 51% to 12–27%. The results suggested that H-bonding between Gln151 of AroG and the inhibitor, L-phenylalanine, had a high impact on L-phenylalanine feedback inhibition. *aroG*^{Q151N} is the good candidate to co-express with genes encoding key enzymes in aromatic amino acid synthetic pathway to obtain the L-phenylalanine overproducing *E. coli* strain.

KEYWORDS: L-phenylalanine, AroG, DAHP synthase, feedback inhibition

INTRODUCTION

L-Phenylalanine is one of the most important aromatic amino acids for humans and animals [1–3]. It is widely used in food and feed industries as, for example, supplementary food and precursor for low calorie sweetener aspartame [4–6]. L-Phenylalanine is also used in pharmaceutical industries for production of pharmaceutically active compounds like HIV protease inhibitor, anti-inflammatory drugs [7], phenylethylamine [8], and catecholamines [9]. Moreover, L-phenylalanine, in combination with UV-C, is used for the production of mulberroside A like resveratrol and rutin [10]; or with UV-A therapy for the treatment of vitiligo [11]. Currently, L-phenylalanine is increasingly in great demand for the production of low-calorie sweetener, aspartame [12, 13]. In early industrial processes, L-phenylalanine was produced by chemical synthesis, which led to various problems and was costly. The synthesis is gradually being replaced with bioprocessing, such as microbial fermentation and enzymatic transformation [14]. More recently, metabolic engineering in *Escherichia coli* has been focused because the main metabolisms of *E. coli* have enabled the introduction of such genetic modifications [15]. Furthermore, genetic engineering technique has been used as another approach to enhance L-phenylalanine yield [16].

The aromatic amino acid biosynthesis pathway in *E. coli* begins with the condensation of phosphoenolpyruvate (PEP) and erythrose 4-phosphate (E4P) to form 3-deoxy-D-arabino-heptulosonate-7-phosphate through the catalysis of DAHP synthase (EC 4.1.2.15). DAHP synthase is the primary target for metabolic regulation by feedback inhibition since each of the three DAHP synthase isozymes is sensitive to regulation by the individual aromatic amino acid end products, L-phenylalanine, L-tyrosine or L-tryptophan [17–19]. About 80% of total DAHP synthase activity is due to AroG, L-phenylalanine-sensitive isozyme. Therefore, the AroG, which is resistant to L-phenylalanine, should solve the mechanism of feedback inhibition and

leads to overproduction of aromatic amino acids through fermentation.

In regard to the 3D structure of AroG co-crystallized with the substrate PEP determined by Shumilin and coworkers in 1999 [20], Hu and colleagues investigated the feedback inhibition site of AroG by amino acid replacement at Phe144, Pro150, Leu175, Leu179, Phe209, Trp215, and Val221. The enzyme activity assay showed that the mutated enzymes completely or partially relieved feedback inhibition of AroG addressed by L-phenylalanine [21].

In 2002, Shumilin and coworkers determined the crystal structure at 2.8 Å of AroG in complex with its inhibitor, L-phenylalanine, PEP, and metal cofactor, Mn^{2+}. Aromatic ring of L-phenylalanine is surrounded by hydrophobic side-chains of Pro150, Gln151, Leu175, Leu179, Phe209, Ser211, Val221, Ile10* (* represents amino acid residue of the companion subunit of the tight dimer), Ile13* and by main-chain atom of Met147, Ile148 and Val212. The carboxylate group of L-phenylalanine is coordinated by O and N of Ser180 and N of Asp7*, while the amino group of the inhibitor interacts with the side-chain oxygen atom of Gln151, as well as Asp6* and Asp7* [22]. In this study, Gln151 was selected for site-directed mutagenesis to determine the effect on L-phenylalanine feedback inhibition of AroG in the attempt to increase L-phenylalanine production.

MATERIALS AND METHODS

Selection of the amino acid residue at L-phenylalanine binding site for mutagenesis

The crystal structure of AroG from *E. coli* complexed with Mn^{2+}, PEP, and L-phenylalanine in the Protein Data Bank with the code 1KFL was used for analysing the amino acid residues that interact with L-phenylalanine at the regulatory site of AroG. BIOVIA Discovery Studio 2020 software (Accelrys Co., Ltd., USA) was used to display the structure.

Plasmids, bacterial strains and culture conditions

All *E. coli* strains and plasmids used in this study are described in Table S1. *E. coli* Top10 was applied for molecular cloning. *E. coli* strains were cultured at 37 °C in LB medium. Antibiotic (kanamycin 30 μg/ml) was added to maintain the plasmids.

Cloning of *aroG*

The *aroG* (1053 bp) was amplified from genomic DNA of *E. coli* JM109 using forward primer (F_AroG_NcoI) containing *Nco*I site and reverse
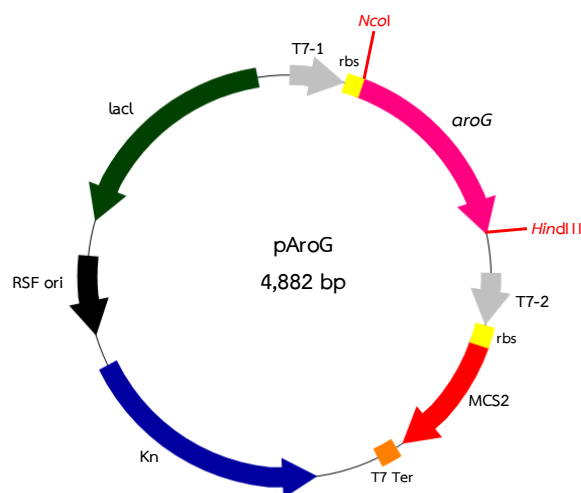
Fig. 1 Map of pAroG. *aroG* from *E. coli* JM109 was inserted into pRSFDuet-1 at *Nco*I and *Hin*dIII sites.

primer (R_AroG_HindIII) containing *Hin*dIII site. The PCR product was cloned into pRSFDuet-1 vector and then transformed into *E. coli* Top10 by electroporation. The recombinant plasmid was confirmed by digestion with *Nco*I and *Hin*dIII. The nucleotide sequencing was performed by Bioneer Inc. (Korea) using ACYCDuetUP1 and DuetDOWN1 primers (Table S2).

Site directed mutagenesis and construction of pAroG^wt and pAroG^fbr

The L-phenylalanine feedback resistant *aroG* (*aroG*^fbr) mutants, Q151A, Q151L and Q151N, were constructed by QuikChange site directed mutagenesis. Each *aroG* mutant gene was amplified using pAroG template and the primers shown in Table S2. After that, the *Dpn*I digestion was performed to cut parental methylated DNA. The plasmids harboring the mutation site (pAroG^fbr: pAroG^Q151A, pAroG^Q151L, and pAroG^Q151N) were verified by the nucleotide sequencing (Bioneer Inc., Korea). The pAroG^wt and pAroG^fbr were transformed into *E. coli* BL21(DE3) and selected on LB agar containing kanamycin 30 μg/ml. The plasmid of each clone was extracted and confirmed by *Nco*I and *Hin*dIII digestion. Map of pAroG is shown in Fig. 1.

Expression of *aroG*

The single colonies of pAroG^wt and pAroG^fbr were separately cultured in 5 ml LB medium containing

30 μg/ml of kanamycin and then incubated with shaking at 37 °C for 16–18 h. A starter was made by inoculating 5% (v/v) of each culture into 50 ml of the same medium and conditions. For shake flask cultivation, the 5% (v/v) of starters were transferred into 200 ml of LB medium and incubated with shaking at 37 °C. After the OD_{600} reached 0.6 (log phase), expression of *aroG* was induced by 1 mM isopropyl-β-D-thiogalactoside (IPTG) for 2 h. The cells of each mutant clone were collected by centrifugation at $8000 \times g$ for 10 min and resuspended in 5 ml of resuspend buffer (0.1 mM potassium phosphate buffer (KPB), pH 7.0, 0.2 mM PEP, 0.5 mM 1,4-dithiothreitol, 0.1 mM phenylmethylsulfonyl fluoride, and 10 mM ethylenediaminetetraacetic acid). The cell pellet of each clone was dissolved in resuspend buffer, and cells were broken by ultrasonic cell disruption. The crude extracts were centrifuged at $10\,000 \times g$ for 20 min to collect the supernatants for dialysis. After dialysis, 1.5 ml of crude extracts was centrifuged at $10\,000 \times g$ for 20 min to collect the supernatant for assay of enzyme activity and SDS-PAGE analysis.

DAHP synthase activity assay

DAHP synthase activity was determined by the method modified from Schoner and Liu [23, 24]. The reaction mixture contained 50 mM KPB, pH 6.5, 5 mM PEP, 2 mM E4P, 0–20 mM L-phenylalanine, crude enzyme, and H_2O in a total volume of 33.75 μl. The mixture was incubated at 30 °C for 10 min. The reaction was initiated when the enzyme was added and stopped by addition of 180 μl of 10% (w/v) trichloroacetic acid. After that, the 45 μl of 25 mM sodium periodate in 62.5 mM sulfuric acid was added to the mixture and incubated at 37 °C for 30 min. Then, 45 μl of 2% (w/v) sodium sulfate in 0.5 M hydrochloric acid was rapidly mixed to stop the reaction; and 450 μl of 0.36% (w/v) thiobarbituric acid was added and mixed. The reaction mixture was boiled for 20 min and then cooled at room temperature. The absorbance at 549 nm was measured by a spectrophotometer. Protein concentration was determined by Lowry's method [25].

SDS-PAGE analysis

The expression of *aroG* was confirmed by SDS-PAGE analysis. The slab gel solution consisted of 12.5% separating gel and 5% stacking gel. For protein loading preparations, the crude enzymes of AroG^{wt} and AroG^{fbr} were mixed with 5x sample buffer (312.5 mM Tris-HCl pH 6.8, 50% (v/v) glycerol and 1% (w/v) bromophenol blue) and boiled for

15 min. After that, the pellets were eliminated by centrifugation at $10\,000 \times g$ for 15 min. The supernatants containing about 100 μg protein were used for SDS-PAGE.

RESULTS AND DISCUSSION

The amino acid residues at L-phenylalanine binding site

The amino acid residues that interact with L-phenylalanine at the regulatory site of AroG are displayed in Fig. 2a. Hydrophobic side chain of L-phenylalanine interacts with Gln151, Leu175, Leu179, Phe209 Ser211, and Ile13* by van der Waals interactions, as well as Pro150, Val221 and Ile10* by pi-alkyl interactions. The carboxylate group of L-phenylalanine forms two H-bonds with Ser180, one H-bond with Asp7* and salt bridge interaction with Arg40; while the amino group forms one H-bond with Gln151 as well as salt bridge interactions with Asp6* and Asp7*. Among these amino acid residues in the regulatory site, Ser180, Gln151, Asp6*, and Asp7*, which can form H-bonds with L-phenylalanine, are interesting.

Ger et al [26] performed random mutagenesis of the cloned *aroG* on a plasmid vector and found that substitution of Ser180 to Phe relieved the degree of feedback inhibition from approximately 60% to less than 10% in the presence of 20 mM L-phenylalanine. Replacement of Phe180 with Ser, Asn and Cys by site-directed mutagenesis demonstrated that Ser180 is a critical residue in the feedback inhibition of AroG.

Recently, Chen et al [27] used a method which integrates CRISPR/Cas9-facilitated engineering of the target gene(s) with growth-coupled and sensor-guided *in vivo* screening (CGSS) to obtain variants of AroG^{fbr} with increased resistance to feedback inhibition of L-phenylalanine. Two residues, Asp6 and Asp7, involved in the L-phenylalanine binding site of AroG were chosen for saturated mutagenesis. They successfully identified several novel L-phenylalanine-resistant AroG variants which exhibited higher specific DAHP synthase activity than that of the reference variant S180F at the presence of 40 mM L-phenylalanine. The replacement of AroG^{S180F} with AroG$^{D6G–D7A}$, which gave the highest specific activity in the L-tryptophan-producing strain, significantly improved the L-tryptophan production by 38.5% (24.03 ± 1.02 g/l at 36 h) in simple fed-batch fermentation.

In 2003, Hu et al [21] investigated the impact of Leu175 on L-phenylalanine feedback inhibition
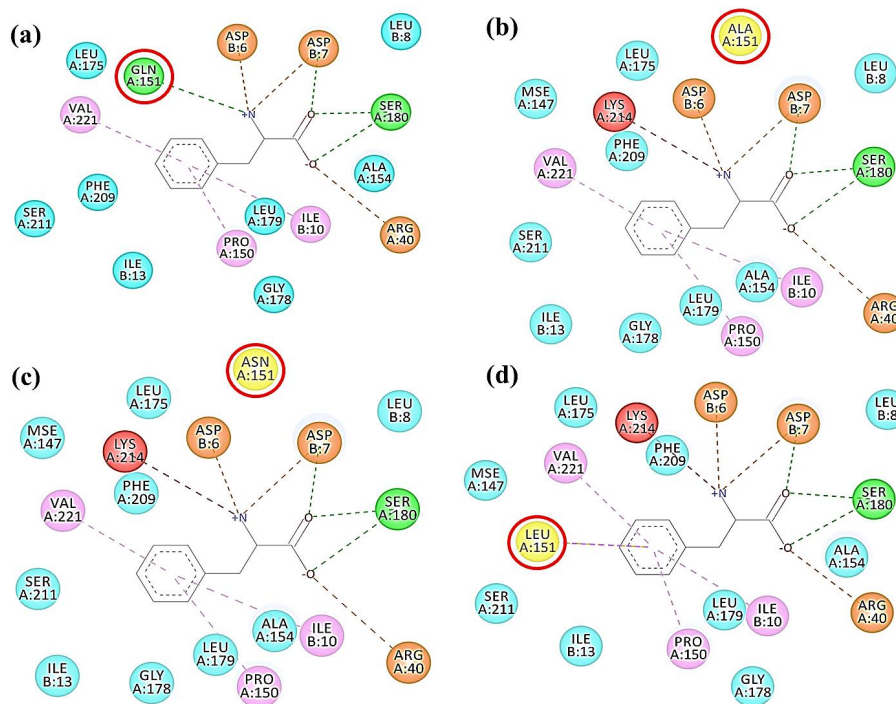
Fig. 2 Amino acid residues that interact with L-phenylalanine at the regulatory site of AroG (a) AroG^{wt}, (b) AroG^{Q151A}, (c) AroG^{Q151N}, (d) AroG^{Q151L}. Red circle represents Q151 and equivalent residues in the mutated enzymes. Yellow color refers to the mutated amino acid residues. Blue, pink, green, red, and orange colors represent the atoms which interact with L-phenylalanine using van der Waals interaction, pi-alkyl interaction, conventional hydrogen bonding, unfavorable donor-donor interaction as well as salt bridge and attractive charge, respectively. The display was made by using the BIOVIA Discovery Studio 2020 software.

by replacement with Ala, Gln and Asp. They concluded that L175D was mostly resistant to feedback inhibition. L175D enzyme elevated specific enzyme activity at 0 mM L-phenylalanine from 2.70 U/mg of wild type to 4.46 U/mg and increased of relative enzymatic activity at 1 mM L-phenylalanine from 8.2% to 83.5%. Surprisingly, in our simulation only van der Waals interaction was found between Leu175 and L-phenylalanine.

In the present study, we are interested in Gln151 because it can form H-bond with L-phenylalanine as well as Ser180, Asp6 and Asp7. No mutation of this residue has never before been reported. Moreover, the pocket accommodating the aromatic ring of L-phenylalanine is formed by hydrophobic side-chains including that of Gln151. To investigate this amino acid residue, structures of AroG when Gln151 was substituted by Ala, Asn and Leu were simulated. We found that all replaced amino acids cannot form H-bond with L-phenylalanine (Fig. 2(b,c,d)). In addition, unfavorable donor-donor interaction occurred between amino groups of L-phenylalanine

and Lys214 of all mutated enzymes. Differ from Ala and Asn, hydrophobic interaction between Leu151 and L-phenylalanine was detected.

Construction of pAroG^{wt} and pAroG^{fbr}

The *aroG* was cloned into pRSFDuet-1 vector and then three *aroG* mutants: Q151A, Q151L and Q151N, were constructed. The recombinant plasmids were confirmed by *Nco*I and *Hin*dIII digestion. Two bands of DNA fragments were observed at 3800 bp and 1100 bp (Fig. 3). DNA sequencing indicated that the sequences of all inserted fragments were correct.

Overexpression of AroG proteins

pAroG^{wt} and pAroG^{fbr} were transformed into *E. coli* BL21(DE3). The transformants were cultured in LB medium and induced with 1 mM IPTG for 2 h. After overexpression, the crude extracts were dialysed to eliminate small molecular weight substances. Then, the expression of *aroG*^{wt} and *aroG*^{fbr} under T7 promoter was evaluated by SDS-PAGE
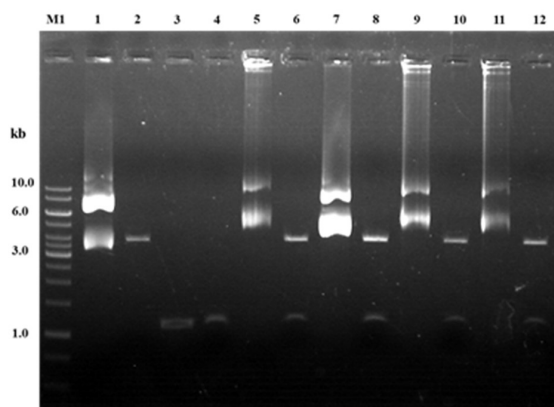
Fig. 3 *Nco*I and *Hin*dIII digestion patterns of pAroG^wt and pAroG^fbr. Lane M1: Gene Ruler 1 kb DNA ladder, Lane 1: uncut pRSFDuet-1, Lane 2: *Nco*I and *Hin*dIII digested pRSFDuet-1, Lane 3: PCR product of *aroG*, Lane 4: PCR product of *aroG* digested with *Nco*I and *Hin*dIII, Lane 5: uncut pAroG^wt, Lane 6: pAroG^wt digested with *Nco*I and *Hin*dIII. Lane 7: uncut pAroG^Q151A, Lane 8: pAroG^Q151A digested with *Nco*I and *Hin*dIII. Lane 9: uncut pAroG^Q151L, Lane 10: pAroG^Q151L digested with *Nco*I and *Hin*dIII. Lane 11: uncut pAroG^Q151N, Lane 12: pAroG^Q151N digested with *Nco*I and *Hin*dIII.
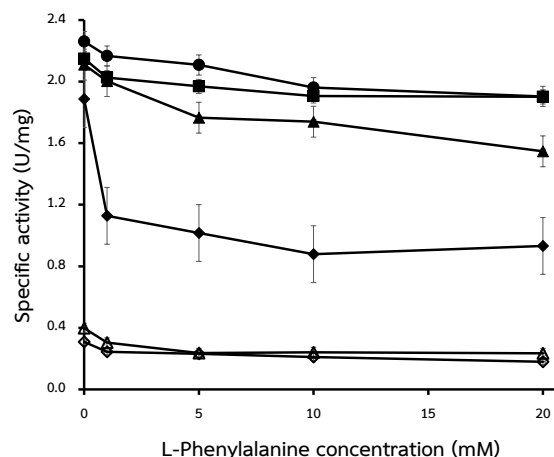
Fig. 5 L-Phenylalanine inhibition patterns of DAHP synthase activities. (◇: *E. coli* BL21(DE3), △: *E. coli* BL21(DE3) harboring pRSFDuet-1, ◆: *E. coli* BL21(DE3) harboring pAroG^wt, ▲: *E. coli* BL21(DE3) harboring pAroG^Q151A, ■: *E. coli* BL21(DE3) harboring pAroG^Q151L and ●: *E. coli* BL21(DE3) harboring pAroG^Q151N). The data were obtained from three independent experiments.

Fig. 4 SDS-PAGE analysis of recombinant AroG in *E. coli*. Lane M, TriColor Protein Ladder (10–180 kDa); Lane 1–3: crude extracts of *E. coli* BL21(DE3), *E. coli* BL21(DE3) harboring pRSFDuet-1, and *E. coli* BL21(DE3) harboring pAroG, respectively.

analysis. As shown in Fig. 4, the crude extracts of *E. coli* BL21(DE3) and *E. coli* BL21(DE3) harboring

pRSFDuet-1 were used as a control (lanes 1 and 2). The band of the recombinant protein was detected after 1 mM IPTG induction for 2 h (lane 3). The size of recombinant protein was approximately 38 kDa.

DAHP synthase activity

DAHP synthase activity of crude extracts from AroG mutants were assayed for sensitivity to feedback inhibition by L-phenylalanine at concentrations from 0 mM to 20 mM. The results are shown in Fig. 5. In the absence of L-phenylalanine, all AroG^fbr clones exhibited 12–20% higher specific activities than that of AroG^wt. This phenomenon was also reported in L8F, S180F [26], F144A, L175A, L175Q, L175D, and F209A [21]. The activities of all recombinant enzymes were decreased in the same pattern when L-phenylalanine was added. All AroG mutants showed greater resistance to feedback inhibition when compared with AroG^wt. AroG^Q151N gave the greatest inhibition pattern; while AroG^Q151A mutant had the lowest inhibition pattern at 0–20 mM L-phenylalanine. Percentages of inhibition by 20 mM L-phenylalanine were decreased from 51% of wild type to 12, 16 and 27% for Q151L, Q151N and Q151A, respectively (Table 1). Destruction of two H-bonding between Ser180 and L-phenylalanine by substitution with Phe (S180F) was reported to decrease the percentage of inhibition

Table 1 DAHP synthase activities and feedback inhibitions of various AroG clones.

Mutant	SA at 0 mM L-phenylalanine (U/mg protein)	SA at 20 mM L-phenylalanine (U/mg protein)	Percentage of inhibition at 20 mM L-phenylalanine (%)
E. coli BL21(DE3)	0.31 ± 0.04	0.18 ± 0.05	42
pRSFDuet-1	0.40 ± 0.07	0.24 ± 0.04	41
AroG^{wt}	1.89 ± 0.39	0.93 ± 0.45	51
AroG^{Q151A}	2.11 ± 0.75	1.55 ± 0.41	27
AroG^{Q151L}	2.15 ± 0.11	1.90 ± 0.05	12
AroG^{Q151N}	2.26 ± 0.06	1.90 ± 0.06	16

SA = specific activity.

by L-phenylalanine at concentration of 20 mM from 58% to 7.4% [26].

In conclusion, the results suggested that H-bonding between Gln151 of AroG and the inhibitor, L-phenylalanine, had a high impact on L-phenylalanine feedback inhibition. Thus, we can use Asn substitution at Gln151 of AroG to increase the enzymatic activity of DAHP synthase especially under high L-phenylalanine concentration.

Appendix A. Supplementary data

Supplementary data associated with this article can be found at http://dx.doi.org/10.2306/scienceasia1513-1874.2021.004.

REFERENCES

1. Liu S, Zhang L, Mao J, Ding Z, Shi G (2015) Metabolic engineering of *Escherichia coli* for the production of phenylpyruvate derivatives. *Metab Eng* **32**, 55–65.
2. Yakandawala N, Romeo T, Friesen A, Madhyastha S (2008) Metabolic engineering of *Escherichia coli* to enhance L-phenylalanine production. *Appl Microbiol Biotechnol* **78**, 283–291.
3. Liu Y, Xu Y, Ding D, Wen J, Zhu B, Zhang D (2018) Genetic engineering of *Escherichia coli* to improve L-phenylalanine production. *BMC Biotechnol* **18**, 1–12.
4. Wu Y, Jiang P, Fan C, Wang J, Shang L, Huang W (2003) Co-expression of five genes in *E. coli* for L-phenylalanine in *Brevibacterium flavum*. *World J Gastroenterol* **9**, 342–346.
5. Baez-vivoros JL, Osuna J, Hernandez-Chavez G, Soberon X, Bolivar F, Gosset G (2004) Metabolic engineering and protein directed evolution increase the yield of L-phenylalanine synthesized from glucose in *Escherichia coli*. *Biotechnol Bioeng* **87**, 516–524.
6. Liu S, Liu R, Xiao M, Zhang L, Ding Z, Gu Z, Shi Y (2014) A systems level engineered *E. coli* capable of efficiently producing L-phenylalanine. *Process Biochem* **49**, 751–757.
7. Weiner M, Albermann C, Gottlieb K, Sprenger GA, Weuster-Botz D (2014) Fed-batch production of L-phenylalanine from glycerol and ammonia with recombinant *Escherichia coli*. *Biochem Eng J* **83**, 62–69.
8. Silkaitis RD, Mosnaim AD (1976) Pathways linking L-phenylalanine and 2-phenylethylamine with *p*-tyramine in rabbit brain. *Brain Res* **114**, 105–115.
9. Khamduang M, Packdibamrung K, Chutmanop J, Chisti Y, Srinophakun P (2009) Production of L-phenylalanine from glycerol by a recombinant *Escherichia coli*. *J Ind Microbiol Biotechnol* **36**, 1267–1274.
10. Pongkitwitoon B, Simpan K, Chobsri T, Sritularak B, Putalun W (2020) Combined UV-C irradiation and precursor feeding enhances mulberroside A production in *Morus alba* L. cell suspension cultures. *ScienceAsia* **46**, 679–685.
11. Siddiqui A, Stolk L, Bhaggoe R, Hu R, Schutgens R, Westerhof W (1994) L-Phenylalanine and UVA irradiation in the treatment of vitiligo. *Dermatology* **188**, 215–218.
12. Ahmad A, David J (2017) Effect of different levels of low-calorie sweetener aspartame on sensory attributes of diabetic Rasgulla. *J Pharm Innov* **6**, 82–84.
13. Zhou H, Liao X, Wang T, Du G, Chen J (2010) Enhanced L-phenylalanine biosynthesis by co-expression of *pheA*^{fbr} and *aroF*^{wt}. *Bioresour Technol* **101**, 4151–4156.
14. Zhang C, Zhang J, Kang Z, Du G, Yu X, Wang T, Chen J (2013) Enhanced production of L-phenylalanine in *Corynebacterium glutamicum* due to the introduction of *Escherichia coli* wild-type gene *aroH*. *J Ind Microbiol Biot* **40**, 643–651.
15. Ikeda M (2006) Towards bacterial strains over-producing L-tryptophan and other aromatics by metabolic engineering. *Appl Microbiol Biotechnol* **69**, 615–626.
16. Wu W, Guo X, Zhang M, Huang Q, Qi F, Huang J (2018) Enhancement of L-phenylalanine production

in *Escherichia coli* by heterologous expression of *Vitreoscilla* hemoglobin. *Biotechnol Appl Biochem* **65**, 476–483.

17. Kikuchi Y, Tsujimoto K, Kurahashi O (1997) Mutational analysis of the feedback sites of phenylalanine-sensitive 3-deoxy-D-arabino-heptulosonate-7-phosphate synthase of *Escherichia coli*. *Appl Environ Microbiol* **63**, 761–762.

18. McCandlis R, Poling M, Herrmann K (1978) 3-Deoxy-D-arabino-heptulosonate 7-phosphate synthase. Purification and molecular characterization of the phenylalanine-sensitive isoenzyme from *Escherichia coli*. *J Biol Chem* **253**, 4259–4265.

19. Niu H, Li R, Liang Q, Qi Q, Li Q, Gu P (2019) Metabolic engineering for improving L-tryptophan production in *Escherichia coli*. *J Ind Microbiol Biotechnol* **46**, 55–65.

20. Shumilin I, Kretsinger R, Bauerle R (1999) Crystal structure of phenylalanine-regulated 3-deoxy-D-arabino-heptulosonate-7-phosphate synthase from *Escherichia coli*. *Structure* **7**, 865–875.

21. Hu C, Jiang P, Xu Jian, Wu Y, Huang W (2003) Mutation analysis of the feedback inhibition site of phenylalanine-sensitive 3-deoxy-D-arabino-heptulosonate-7-phosphate synthase of *Escherichia coli*. *J Basic Microbiol* **43**, 399–406.

22. Shumilin I, Zhao C, Bauerle R, Kretsinger R (2002) Allosteric inhibition of 3-deoxy-D-arabino-heptulosonate-7-phosphate synthase alters the coordination of both substrates. *J Mol Biol* **320**, 1147–1156.

23. Schoner R, Herrmann K (1976) 3-Deoxy-D-arabino-heptulosonate 7-phosphate synthase purification, properties, and kinetics of the tyrosine-sensitive isoenzyme from *Escherichia coli*. *J Biol Chem* **251**, 5440–5447.

24. Liu Y, Li P, Zhao K, Wang B, Jiang C, Drake H, Liu S (2008) *Corynebacterium glutamicum* contains 3-deoxy-D-arabino-heptulosonate 7-phosphate synthases that display novel biochemical features. *Appl Environ Microbiol* **74**, 5497–5503.

25. Lowry O, Rosebrough N, Farr A, Randall R (1951) Protein measurement with the folin phenol reagent. *J Biol Chem* **193**, 265–275.

26. Ger Y, Chen S, Chiang H, Shiuan D (1994) A single Ser-180 mutation desensitizes feedback inhibition of the phenylalanine-sensitive 3-deoxy-D-arabino-heptulosonate 7-phosphate (DAHP) synthetase in *Escherichia coli*. *J Biochem* **116**, 986–990.

27. Chen M, Chen L, Zeng A (2019) CRISPR/Cas9-facilitated engineering with growth-coupled and sensor-guided *in vivo* screening of enzyme variants for a more efficient chorismate pathway in *E. coli*. *Metab Eng Commun* **9**, ID e00094

Appendix A. Supplementary data

Table S1 Bacterial strains and plasmids used in this study.

Strain/Plasmid	Characteristic	Source/Reference
Strain		
E. coli BL21(DE3)	F–*omp*T *hsdS*$_B$ (r$_B$–, m$_B$–) *gal dcm* (DE3)	Novagen
E. coli JM109	F′ *traD*36 *proA$^+$B$^+$ lacI*^{q} Δ(*lacZ*)*M15*/Δ(*lac-proAB*) *glnV44 e14- gyrA96 recA1 relA1 endA1 thi hsdR17*	Novagen
E. coli Top10	F– *mcrA* Δ(*mrr-hsdRMS-mcrBC*) φ80*lacZ*ΔM15 Δ*lacX74 recA1 araD139* Δ(*ara-leu*) 7697 *galU galK* λ— *rps*L(Str^R) *end*A1 *nup*G	Invitrogen
Plasmid		
pRSFDuet-1	pRSF1030 replicon, T7 promoter expression vector, *lacI*, Kan^r	Novagen
pAroG^{wt}	pRSFDuet-1 inserted with *aroG*^{wt} under the control of T7 promoter	This study
pAroG^{Q151A}	pRSFDuet-1 inserted with *aroG*^{Q151A} under the control of T7 promoter	This study
pAroG^{Q151L}	pRSFDuet-1 inserted with *aroG*^{Q151L} under the control of T7 promoter	This study
pAroG^{Q151N}	pRSFDuet-1 inserted with *aroG*^{Q151N} under the control of T7 promoter	This study

Table S2 The sequences of oligonucleotide primers for PCR amplification, DNA sequencing and site-directed mutagenesis in this study.

Primer	Sequence	T_w (°C)
For PCR amplification and DNA sequencing		
F_AroG_NcoI	5′–CATGCCATGGTGTATCAGAACGACGATTTACGCATCAAAGAAATC–3′	61.4
R_AroG_HindIII	5′–CCAAGCTTTTACCCGCGACGCGCTTTCACTGC–3′	67.2
ACYCDuetUP1	5′–GGATCTCGACGCTCTCCCT–3′	60.0
DuetDOWN1	5′–GATTATGCGGCCGTGTACAA–3′	57.0
For Site-directed mutagenesis		
F_5′ Q151A	5′–GGTGAATTCCTCGATATGATCACTCCTGCCTATCTCGCTGACCTGATGAGCTGGGGC–3′	75.4
R_3′ Q151A	5′–GCCCCAGCTCATCAGGTCAGCGAGATAGGCAGGAGTGATCATATCGAGGAATTCACC–3′	75.4
F_5′ Q151L	5′–GGTGAATTCCTCGATATGATCACTCCTCTGTATCTCGCTGACCTGATGAGCTGGGGC–3′	74.7
R_3′ Q151L	5′–GCCCCAGCTCATCAGGTCAGCGAGATACAGAGGAGTGATCATATCGAGGAATTCACC–3′	74.7
F_5′ Q151N	5′–GGTGAATTCCTCGATATGATCACTCCTAATTATCTCGCTGACCTGATGAGCTGGGGC–3′	73.2
R_3′ Q151N	5′–GCCCCAGCTCATCAGGTCAGCGAGATAATTAGGAGTGATCATATCGAGGAATTCACC–3′	73.2